Influence of Alkyl Chain Length of 1,3-Bis-Dialkylamino-2-Propanol on the Adsorption and Corrosion Behavior of Steel Q235 in Simulated Concrete Pore Solution

J. Cai[*]*, C. Chen, J. Liu, W. Zhou, J. Liu*

State Key Laboratory of High Performance Civil Engineering Materials, Jiangsu Research Institute of Building Science, Nanjing 211103, China
[*]E-mail: caijingshun@gmail.com

A set of four linear alkyl chain 1,3-bis-dialkylamino-2-propanol (2-2OH-2, 4-2OH-4, 6-2OH-6, 8-2OH-8), were used in this work to evaluate the effect of carbon chain length on the adsorption and corrosion behavior of steel Q235 in simulated concrete pore solution containing 0.3 mol/L NaCl by electrochemical techniques, XPS and quantum chemical calculations. The results showed that n-2OH-n (n=2,4,6,8) were anodic inhibitor and inhibition efficiency of n-2OH-n (n=2,4,6,8) ranked as 8-2OH-8>6-2OH-6>4-2OH-4>2-2OH-2. With adsorbing atoms and length of non-polar carbon chains of n-2OH-n (n=2,4,6,8) increased, corrosion current density decreased and pitting expansion was restrained effectively. 8-2OH-8 can form a compact adsorption film according to Langmuir adsorption isotherm and standard free energy of adsorption (ΔG_{ads}^{0}) is -40.97 kJmol⁻¹. According to frontier orbital theory, n-2OH-n (n=2,4,6,8) can adsorb on substrate mainly by nitrogen atom and form a compact barrier layer by non-polar radicals overlap on surface of electrode.

1. INTRODUCTION

Corrosion of steel bars is one of the most serious problems in reinforced concrete structures and became of great interest at the end of 80's and early 90's since its elevated economic and social impact was pointed out. For preventing reinforcing steel from corrosion attack, there are many alternative approaches can be used, while usage of corrosion inhibitor seem to be attractive because of their low cost and easy handling. [1-4]

Widely recognized is that nitrite based inhibitors are the most effective in concrete system compared with other inorganic corrosion inhibitors, such as sodium mono-fluoro-phosphate,

molybdate, zinc oxide and so on. However, environmental limitations have highly reduced its usage nowadays.[5-8]

For these reasons, organic inhibitors, which are typically base on the mixtures of amines and amino alcohols or an emulsion of unsaturated fatty acid ester, were widely studied.[9-12] The most efficient organic inhibitors are compounds with functional groups containing oxygen, nitrogen or sulphur, which have the ability to form complexes with iron or forming an adsorbed film on metal surface.[13-16] Among these organic inhibitors, traditional amino alcohol is one of the most widely investigated but conflicting opinions obtained.[9-15,17-23] Most of investigations and literatures reveal that amino alcohol can delay the onset of corrosion of reinforcing steel, but cannot reduce the corrosion rate when the corrosion of rebar have began.[9, 15, 17, 18, 19, 24] Moreover, these traditional amino alcohols are mono-nitrogen atom and relatively short carbon chain, employed in field engineering have following problems: cannot elevate chloride threshold level, high volatility caused wastage during long time, inhibition efficiency cannot exceed nitrite when usage of amino alcohol only. [9, 17, 19, 25] Recently, Zhou and Dong find that some compounds with muti-hydroxyl and multi-amine can form iron chelate compounds and inhibit corrosion of carbon steel.[26, 27] Beside, steric effect of organic structure also largely influences the inhibition efficiency.[15] So, the organic inhibitor structure with relatively more adsorption atoms and suitability non-polar carbon chain or aromatic ring will increase the capability of adsorbed film and form an intensity barrier layer resisting corrosion ion attack.

In present work, some compounds of 1,3-bis-dialkylamino-2-propanol shown in Table 1 with two N atom and different length of alkylic electron donating chain was prepared for increasing the negatively charge of N atom and the steric barrier to Cl^- to improve the corrosion resistance of carbon steel. These amino-alcohols had been investigated as Vapor Corrosion Inhibitor (VCI) for corrosion resistance of brass and the carbon steel in thin electrolyte layer and demonstrated extraordinary inhibition efficiency.[28, 29] However, the corresponding amino-alcohols used as inhibitor for carbon steel in concrete pore solution have nearly been investigated yet, and there is not essential information available to understand their inhibition mechanism.

The purpose of this work is to investigate the influence of carbon chain length of these amino-alcohols on the inhibition efficiency and adsorption property in chloride contaminated simulated concrete pore solution. The electrochemical performance of carbon steel electrode was investigated by potentialdynamic polarization and electrochemical impedance spectroscopy (EIS). The adsorption properties and surface composition of steel sample was evaluated via X-ray photoelectron spectroscopy (XPS) as well in order to verify the presence of inhibitor on the carbon steel surface. The adsorption behavior and corrosion inhibition mechanism were also analysis according to frontier orbital theory.

2. EXPERIMENT WORK

2.1 Materials and sample preparation

The series of amino alcohols, n-2OH-n (n=2,4,6,8), were prepared according the reference[28-30] and structure were all shown in Table 1.

Table 1. Structure of n-2OH-n (n=2,4,6,8)

Sample	Molecular structure	Molecular formula	Symbol
I		$C_7H_{18}N_2O$	2-2OH-2
II		$C_{11}H_{26}N_2O$	4-2OH-4
III		$C_{15}H_{34}N_2O$	6-2OH-6
IV		$C_{19}H_{42}N_2O$	8-2OH-8

The blank of simulated concrete pore solution are saturated calcium hydroxide adding 0.01 mol/l sodium hydroxide to adjust pH to 12.6 with 0.3mol/L sodium chloride to simulate the chloride-contaminated concrete system. The blank solution containing 3.6g/L n-2OH-n (n=2,4,6,8) were prepared to compare chain length change on corrosion behavior of carbon steel.

2.2 Electrochemical measurements

Table 2. Chemical composition of Q235 steel

Content,%	C	Mn	Si	S	P	Fe
	0.22	1.4	0.35	0.05	0.045	balance

The working electrodes were cut from carbon steel bar (No. Q235 according to GB/T 221-79). Its composition was listed in Table 2. Connected a copper wire to one side of the steel and submerged it into epoxy resin leaving an exposed working area of 1 cm². Before test, the electrodes were grinded gradually with SiC paper (grade 240#, 400#, 1000# and 2000#), and then degreased and rising with ethanol, all the experiments were performed three times and kept all the experiments reproducibility.

For electrochemical measurements, a three-electrode cell was used, consisting of a saturated calomel reference electrode (SCE), a platinum foil counter electrode, and the prepared working electrode. All the electrochemical experiments were carried out using 273A (Princeton Applied Research) with a 5210 lock-in amplifier. Potentiodynamic polarization curves were conducted at a sweep rate of 0.5 mV/s from −200 mV to 800 mV versus the open circuit potential (OCP) after the electrodes were immersed in test solution for 0.5 h. EIS was performed at the OCP in the frequency

range of 100 kHz-10 mHz with a 10 mV amplitude signal after the electrodes were immersed in test solutions for 0.5h.

2.3 XPS analysis

The steel disk was immersed in control solution with 0.3 mol/l sodium chloride and 3.6g/L 8-2OH-8 at 25℃ for 4 days. After removal from the cell, the disk was rinsed with deionized water and dry in infrared lamp. Surface analysis was performed with PHI5000 VersaProbe. The X-ray source was monochromatised Al Ka ray of 1486.6eV under pressure below 10^{-6} Pa. Sputtered area of 0.5mm×0.5mm was analyzed. Ar^+ sputter energy 4 kV，sputtering rate is 46nm/min, and sputtering time is 0.1min and 0.2 min, respectively. The following sequence of spectra was recorded: C 1s, O 1s, N 1s and Fe 2p. The binding energy scale was set by fixing the C 1s component due to carbon only bound to carbon and hydrogen at 284.8 eV. The data treatment was performed with the XPSPEAK software. The peaks were decomposed using a Shirley baseline.

3. RESULTS

3.1. ELECTROCHEMICAL MEASUREMENTS

3.1.1. Potentiodynamic polarization
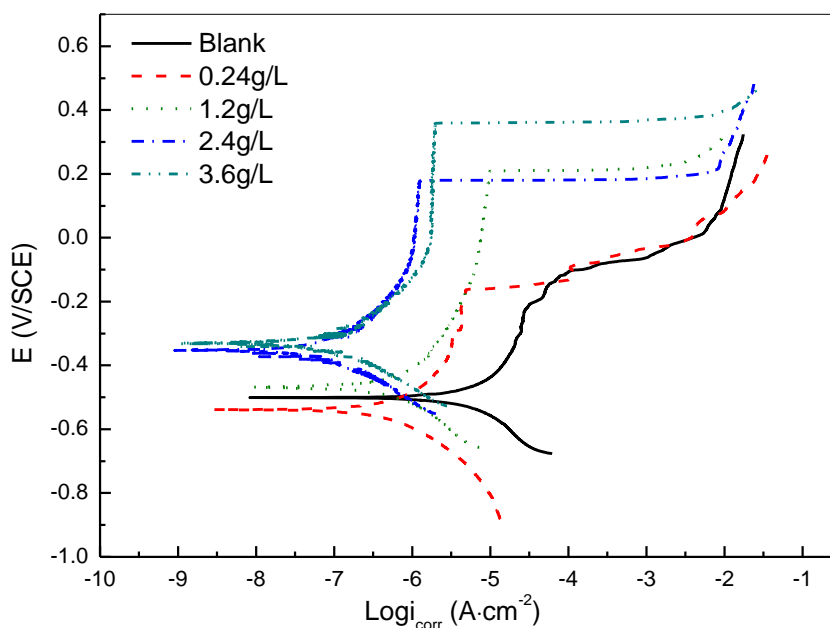
Figure 1. Potentiodynamic polarization curves for carbon steel in simulated concrete pore solution with different concentration of 8-2OH-8

Fig. 1 depicts polarization curves for carbon steel in blank solution with different concentrations of 8-2OH-8. It can be seen that the anodic process of carbon steel corrosion was effectively retarded by the inhibitor, and these effect became more pronounced with increasing inhibitor concentrations, while the corrosion potential move positively with concentration increased. These results indicate that 8-2OH-8 has a stronger inhibition effect on the anodic dissolution of iron, which can be considered as an anodic inhibitor.

It also can be seen that after the addition of the inhibitor, the anodic polarization curves showed a significant shift of the broken potential in positive direction and a wider passive region in comparison with that in blank solution. These results suggest that the pitting corrosion was strongly suppressed by the inhibitor.

Table 3. The electrochemical parameters obtained from potentiodynamic polarization measurements presented in Fig. 1

Conc.	E_{corr}	E_b	E_b-E_{corr}	i_{corr}	η	θ
g/L	mV	mV	mV	$\mu A \cdot cm^{-2}$	%	
Blank	-501	-192	309	1.12	-	-
0.24	-551	-165	286	0.19	83.6	0.836
1.2	-469	205	674	0.11	90.1	0.901
2.4	-362	179	541	0.013	98.8	0.988
3.6	-346	359	705	0.006	99.4	0.994

The relevant fitted electrochemical parameters (i_{corr}, E_{corr}, E_b, E_b-E_{corr}, η, θ) from polarization curve in vicinity of potential ($E_{corr} \pm 20mV$) are shown in Table 2. E_{corr} was corrosion potential and film broken potential respectively. E_b was defined as the potential at which anodic current density started to increase abruptly, which demonstrated the broken of passive film. E_b-E_{corr} was the width of the passive range, calculated from the difference between E_b and E_{corr}. The inhibition efficiency (η) was calculated by the follow equation:[27]

$$\eta = \frac{i_{corr}^o - i_{corr}}{i_{corr}^o} \times 100 \qquad (1)$$

where i_{corr}^o and i_{corr} were corrosion current density of carbon steel in solution before and after adding inhibitor, respectively.

It was evident that the increase of 8-2OH-8 concentration would result in a decrease of corrosion current density and an increase of passive range and inhibition efficiency. When concentration of 8-2OH-8 is 3.6g/L, the inhibition efficiency is largest at 99.4%. So 3.6g/L corrosion inhibitor are selected for different chain length of amino-alcohols, n-2OH-n (n=2, 4, 6, 8), measured by potentiodynamic polarization curve. Potentiodynamic polarization curves and fitted electrochemical parameters are presented in Fig. 2 and Table 4, respectively.
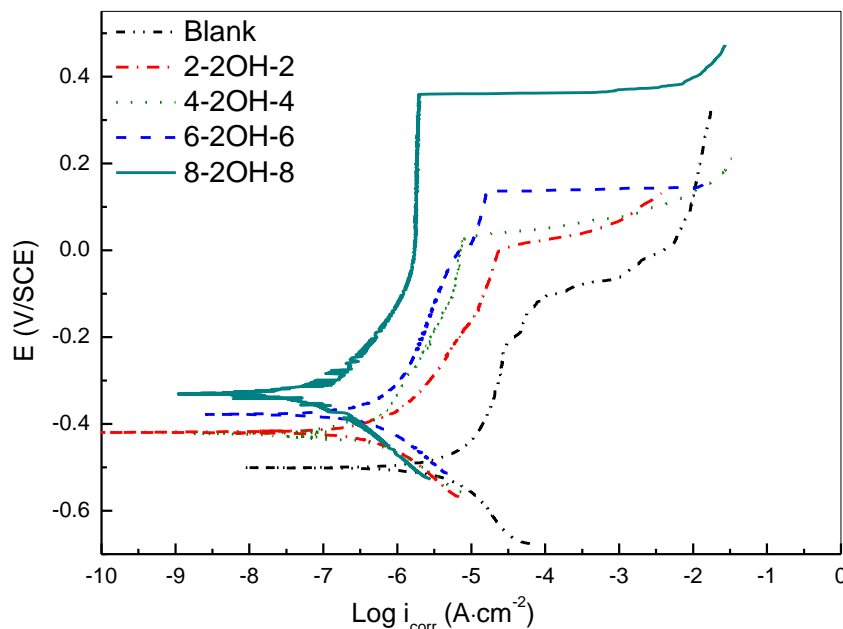
Figure 2. Potentiodynamic polarization curves for carbon steel in simulated concrete pore solution without and with n-2OH-n (n=2,4,6,8)

Fig. 2 shows that the corrosion potential shifts more positive and passive range becomes wider with the length of carbon chain increase, and Table 4 shows that corrosion current density decrease and inhibition efficiency increase with carbon chain length increase. This suggests that a more and more complete and stable barrier film was forming on the steel surface. It also indicates that the non-polar carbon chain increase, the barrier layer are more intensity.

Table 4. The electrochemical parameters obtained from potentiodynamic polarization measurements presented in Fig. 2

Sample	E_{corr} mV	E_{pit} mV	$E_{pit}-E_{corr}$ mV	i_{corr} $\mu A \cdot cm^{-2}$	η %
Blank	-501	-112	389	1.12	-
2-2OH-2	-419	-5	414	0.12	89.3
4-2OH-4	-422	34	456	0.10	91.1
6-2OH-6	-378	138	516	0.016	98.6
8-2OH-8	-329	359	688	0.006	99.4

3.1.2. Electrochemical impedance

Fig. 3 disclose the EIS plots of carbon steel traced at OCP in 0.3mol/L NaCl simulated concrete pore solution with n-2OH-n (n=2, 4, 6, 8). The result shows that the impedance value in low frequency and the maximum phase angle both increased with carbon chain length. Carbon chain length increase large enough, the phase angle shift toward to low frequency and another phase angle clearly observed.

This is probably due to the nearly intact barrier of n-2OH-n (n=2, 4, 6, 8) on the metal surface with carbon chain length increase. This barrier film can effectively prevent chloride ion and oxygen close to metal surface.
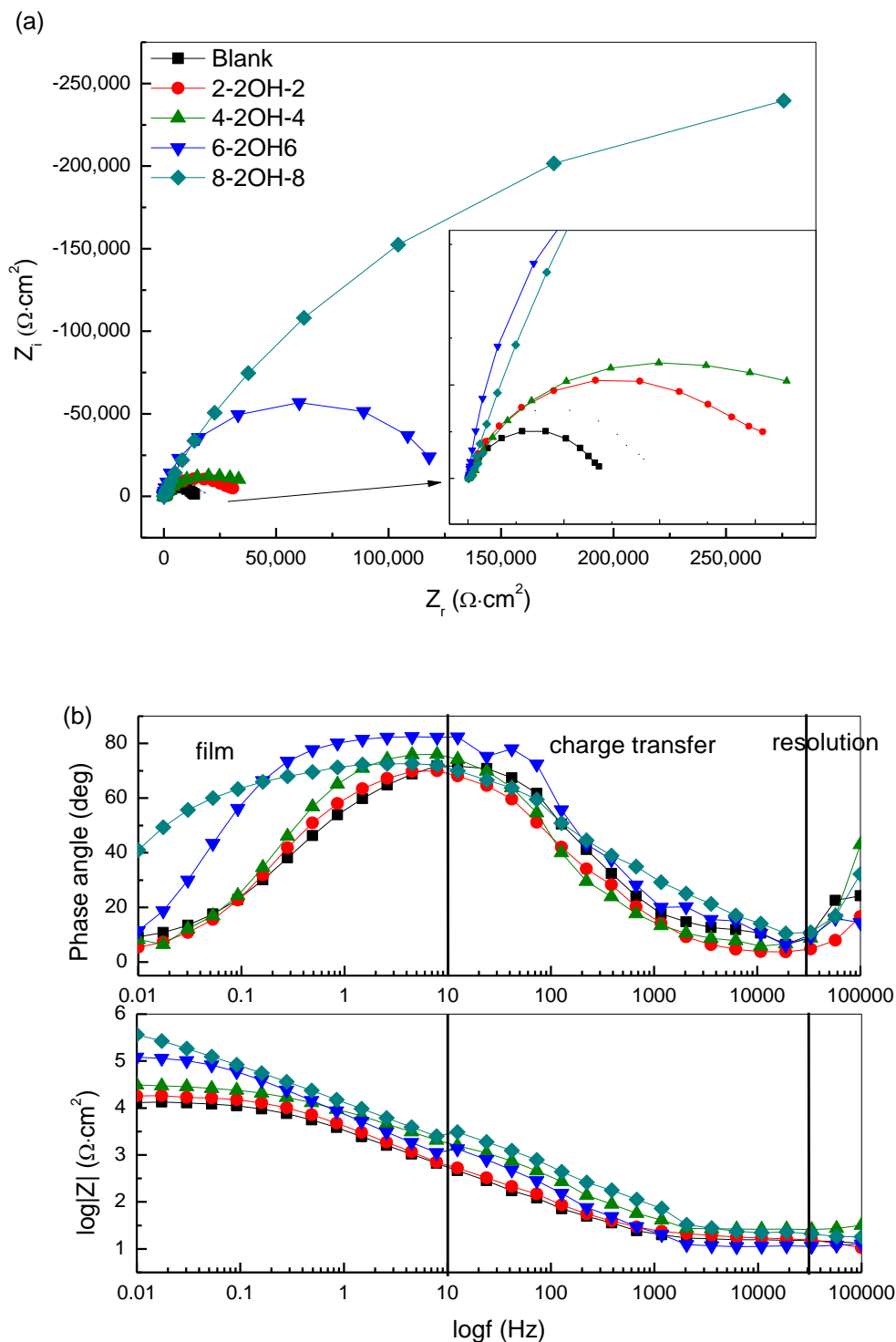
Figure 3. EIS for carbon steel in simulated concrete pore solution without and with n-2OH-n (n=2,4,6,8) (a) Nyquist plots, (b) Bode plots
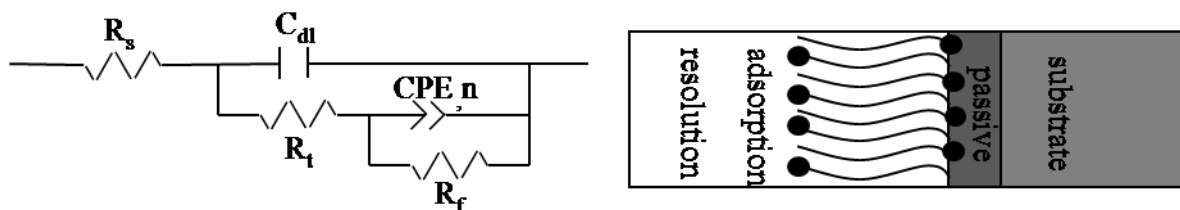
Figure 4. Electrochemical equivalent circuit

Besides, Fig. 3 (b) presents two maximum phase lags, indicating two time constant, which can be attributed to the resistance and capacitance of passive film at low frequency and the resistance of charge transfer and capacitance of electric double layer at higher frequency. Corresponding equivalent circuit is shown in Fig. 4. Where, R_s is the solution resistance, R_t is the charge transfer resistance, C_{dl} is double layer capacitance, R_f is film resistance. Constant phase element (CPE) is instead of pure film capacitance (C_f). $Z(CPE)=[Q(j\omega)^n]^{-1}$, where Q is the constant, ω is the angular frequency, and n is the CPE power, which is an adjustable parameter that usually lies between 0.5 and 1, when n=0.5, it is the Warburg resistance, n=1, is the ideal capacity. The present of the CPE is due to distributed surface heterogeneity, roughness, fractal geometry, electrode porosity and to current and potential distributions related with electrode geometry.[32,33] The fitted results of the experiment data by the proposed equivalent circuit are also shown in Table 5.

Table 5. The electrochemical parameters obtained from EIS presented in Fig. 3

Sample	R_s $\Omega \cdot cm^2$	C_{dl} $\mu F \cdot cm^{-2}$	R_t $K\Omega \cdot cm^2$	C_f $\mu F \cdot cm^{-2}$	n	R_f $K\Omega \cdot cm^2$
Blank	16.27	11.97	4.51	53.41	0.79	11.60
2-2OH-2	28.62	7.81	16.35	26.45	0.72	28.32
4-2OH-4	26.70	7.65	17.51	33.10	0.79	32. 03
6-2OH-6	12.17	7.21	19.50	16.01	0.92	113.80
8-2OH-8	22.90	2.90	38.36	16.00	0.91	402.41

It is apparent from Table 5 that by increasing carbon chain length, the C_{dl} and C_f values tended to decrease, whereas the R_t and R_f increase. The significant decrease in the capacitance values can be ascribed to a decrease in the dielectric constant or an increase in the double electric layer thickness due to the adsorption of inhibitor molecule on carbon steel surface. Usually, in blank solution, H_2O, OH^- and Cl^- may adsorb on electrode surface.[24,26] After adding organic corrosion inhibitor, which may adsorb on electrode surface and replace the H_2O, O_2, OH^- and Cl^-. The remarkable increase in R_t demonstrates that the inhibitor adsorb on electrode can effectively retard the corrosion reaction. That because of the carbon chain length increase, the water repellent ability more strong, the transport of H_2O, O_2 and Cl^- to surface electrode more difficult, then the charge transfer and film resistant increase.

3.2. Adsorption analysis

3.2.1 Surface analysis
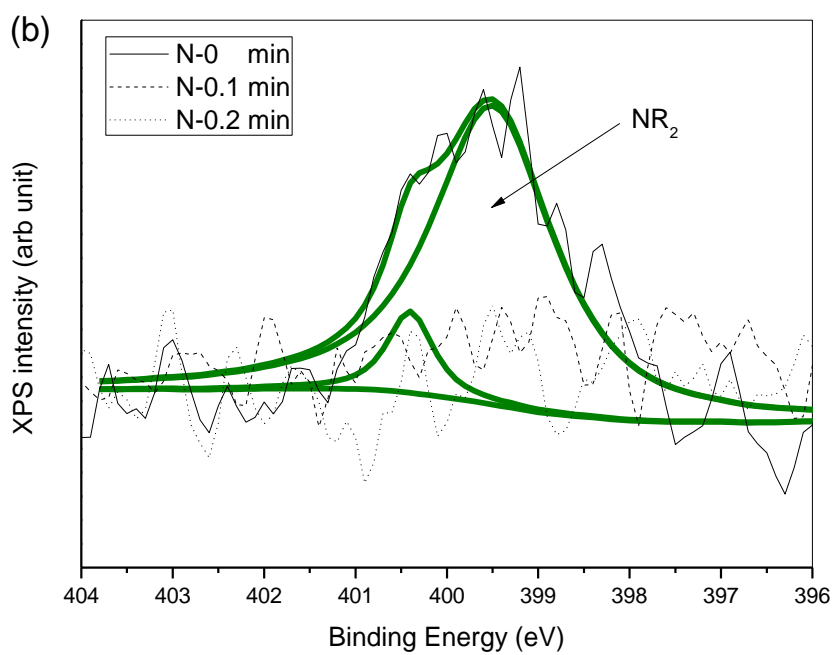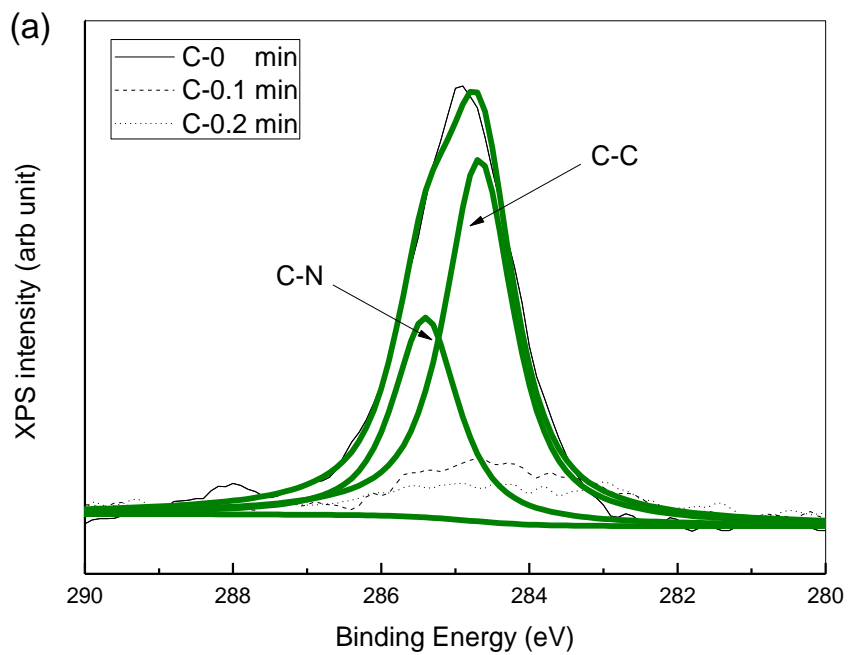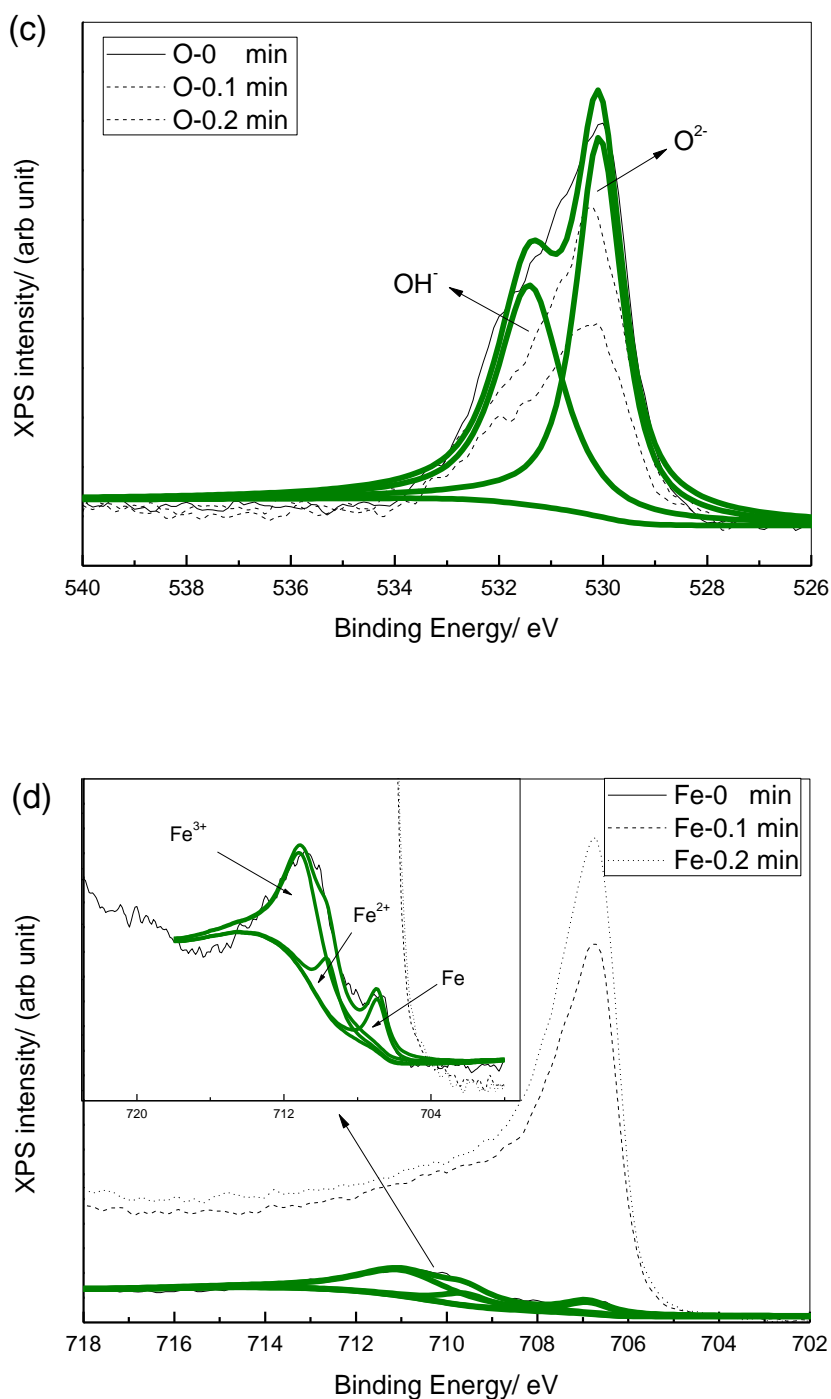
Figure 5. Depth profile XPS spectra for carbon steel sample exposed to simulated concrete pore solution with 8-2OH-8: (a) C 1s (b) N 1s (c) O 1s (d) Fe 2p3/2

Fig. 5 disclose the depth profile of spectral for C, N, O and Fe on the carbon steel surface and sputtering surface 0.1min and 0.2min. It can be found that the deconvoluted XPS spectral of C 1s show two peaks before sputtering (Fig. 5(a)). The peak at 284.5eV and 285.4eV were assigned to C-C and C-N, respectively. The binding energy of the two decomposed peaks was 399.5eV and 400.4eV (Fig.

5(b)), which was attributed to N-C in amide and amine or deprotonated amine group, R3N.[34,35] Furthermore, as depicted in Fig. 5(c), there are two peaks at 530.5eV and 532.3eV, which are ascribed to O^{2-} and OH^-. And the XPS spectral of Fe $2p_{3/2}$ shows three peaks. The peak at 706.9 eV was assigned to metallic Fe. The ferrous compounds and ferric compound appear at 709.2 eV and 710.9 eV, respectively.[27,37] After sputtering, these peaks in Fig. 5 (a), (b) and (c) all disappear, while only a peak of metallic Fe emerged at 706.9eV. These were a convincing evidence for the adsorption of 8-2OH-8 on the surface of steel after 4 days of immersion.

3.2.2 Isothermal Adsorption
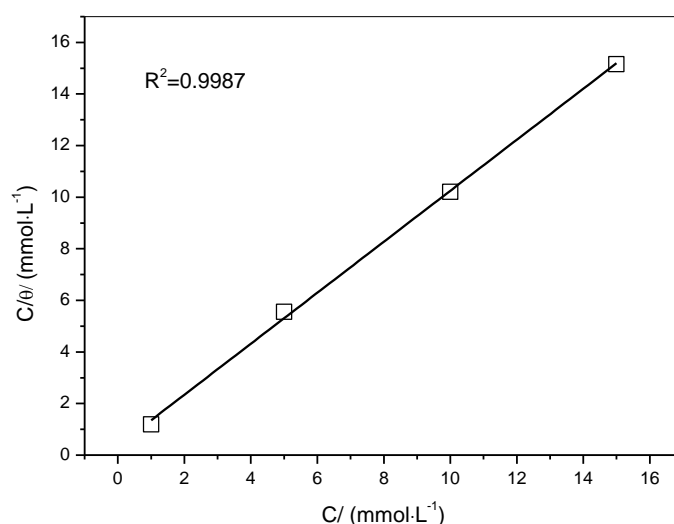
Figure 6. Langmuir adsorption isotherm plots for steel Q235 in simulated concrete pore solution containing 8-2OH-8

For further understanding the interaction mechanism between organic molecules and metal surface, the adsorption isotherm was employed. In present investigation, the data obtained from polarization measurements fitted well with Langmuir isotherm, as shown in Fig. 6. According to Langmuir isotherm, θ was related to inhibitor concentration as:[16,27]

$$\frac{C}{\theta} = \frac{1}{K_{ads}} + C \qquad (1)$$

Where θ is the surface coverage of the inhibitor on the steel surface and was equal to the inhibition efficiency. C is the concentration of 8-2OH-8 and K_{ads} is the adsorption equilibrium constant. The intercepts of the C/θ versus C line is adopted to calculate the adsorption equilibrium constant. The standard adsorption free energy (ΔG^0_{ads}) is estimated from Equation 2:

$$\log K_{ads} = \log \frac{1}{55.5} - \frac{\Delta G_{ads}^{O}}{2.303RT} \qquad (2)$$

Where the numeral of 55.5 is the molar concentration of water in solution, R is the universal gas constant and T is the absolute temperature (298K in this study).

The K_{ads} values could be taken as a measure of the strength of the adsorption forces between the inhibitor molecules and the metal surface. The higher value of K_{ads} revealed that the inhibitor performed stronger adsorption ability onto the steel surface. ΔG_{ads}^{0} value was an expression of adsorption character. As reported, ΔG_{ads}^{0} value of -20 kJmol^{-1} or higher indicated a physical adsorption, while that of more negative than -40 kJ mol^{-1} involved sharing or transferring of electron from the inhibitor molecules to the metal surface to form a coordinate type bond (chemical adsorption).[16,27] The calculated adsorption equilibrium constant (K_{ads}) was 2.75×10^{5} mol^{-1} and ΔG_{ads}^{0} was -40.97 kJmol^{-1}. According to these, the adsorption of 8-2OH-8 on steel surface is chemical sorption.

4. DISCUSSION
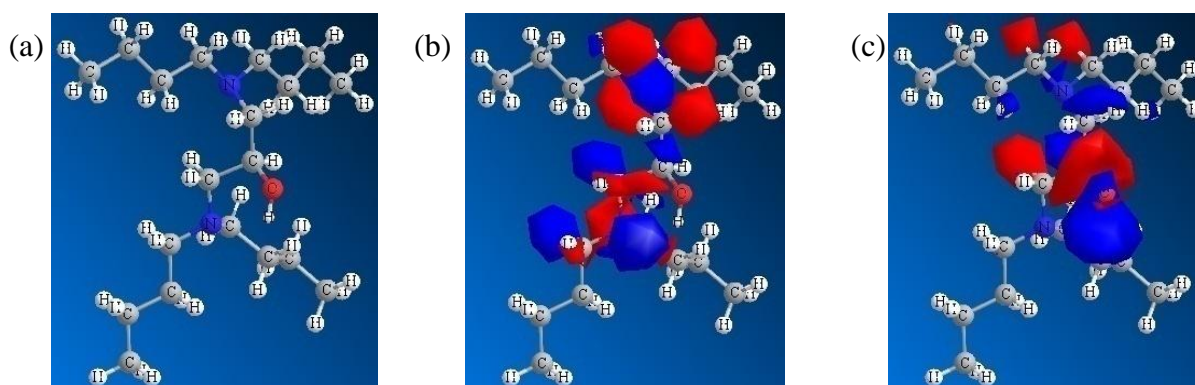
Figure 7. Optimization molecular structure and the frontier molecular orbital density distribution for 8-2OH-8: (a) optimized molecular structure; (b) HOMO (the highest occupied molecular orbital); (c)LUMO(the lowest unoccupied molecular orbital)

Since chemisorptions was heteroatom interact with electrode surface. However, there were two kinds of heteroatom. In order to further understanding this adsorption process, quantum chemical calculations were performed by Gaussian 09W with DFT method.[38,39] The optimized molecular structure of the 8-2OH-8 and molecular orbital distribution of HOMO and LUMO are depicted in Fig. 7. It can be seen that the HOMO was located near the N atom due to the strong sharing electron ability, while LUMO was mainly distributed on the O atom. According the molecular orbital theory, the HOMO orbital can offer electron, while Fe 3d orbital is short of electron.[37,38] When inhibitor nears the surface of carbon steel, N atom will interaction with Fe atom and form chemical bond. Then non-polar carbon chain will over electrode surface and formed a barrier layer to repelled corrosion ions attack.
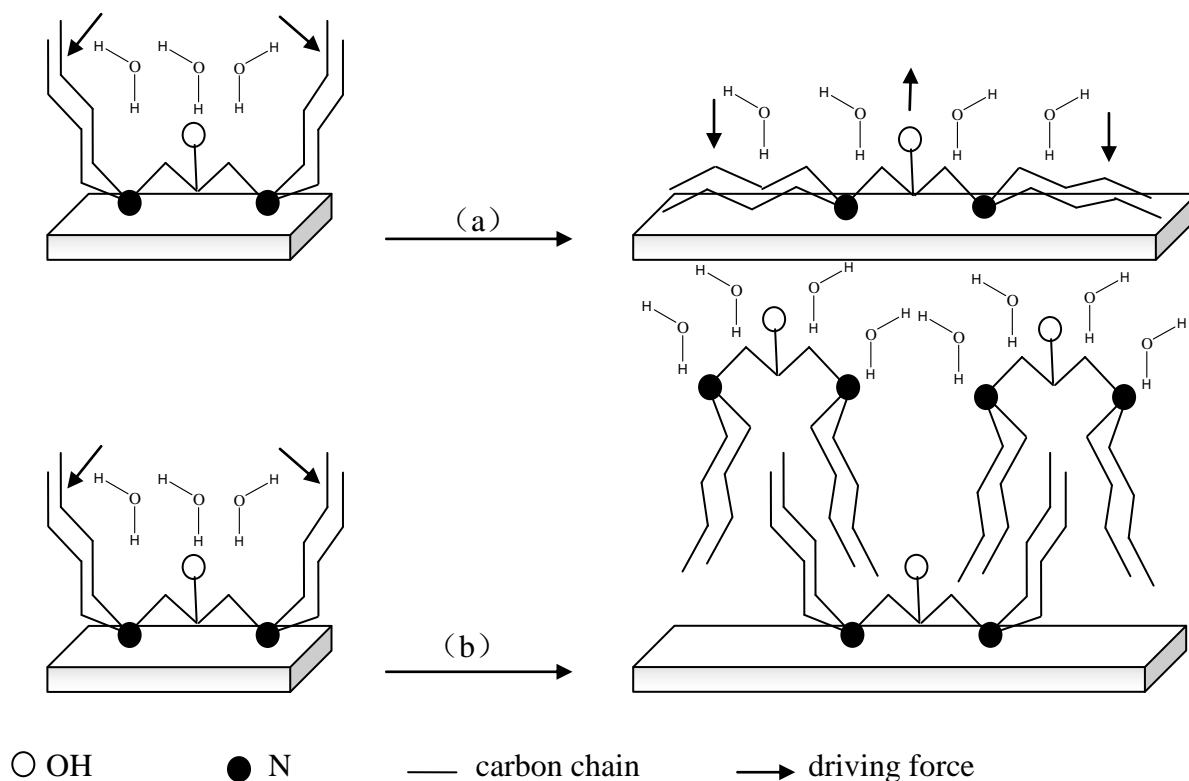
Figure 8. Possible orientation of inhibitor on the metal stripe surface and corrosion

After N atom interacts with Fe atom, the long carbon chain will over electrode surface and exposure in solution. As is well known that the long carbon chain is non-polar radical, H_2O is polar molecular. When carbon chain is sufficient long, the H_2O cannot resolution it. For decreasing potential energy, the surface tension may drive the long carbon chain out of solution to electrode surface at the interface of electrode/solution. This process is shown in Fig. 8 (a). But this adsorption process was not a very stable process. When the inhibitor concentration is enough, there may be another adsorption film form, which is shown in Fig.8 (b). According polarity compatible, the non-polar carbon chain will interlock and the polar radical will exposure into solution. The hydrocarbon tails mesh with each other in a sort of "Zipper" effect to form a tight film which can effectively repel aqueous fluids, establishing a barrier to the chemical and electrochemical attack of fluids on the base metal.[12] When this process achieves an equivalent, a more thick, intensity and stable adsorption film will form.

However, this film formation process was also a competitive process with Cl^- OH^- and H_2O. Higher corrosion resistance was probably the indication of higher adsorption ability and steric effect of the hydrophobic side chains. The results shows that long hydrophobic chain increase the electron of N atom and steric effect to increase adsorption ability and film intensity.

For short carbon chain length of amino-alcohols, the barrier film was not intensity, cannot completely retard the H_2O and Cl^-, so inhibition efficiency increase with carbon chain length. Besides, there may be another corrosion mechanism for shorter length amino-alcohols.

As well known that organic amines are basic compounds, which can hydrolyze and following equation occur:

$NR_3+H_2O=HN^+R_3 +OH^-$
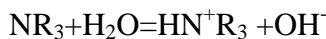
On the carbon steel surface, the reduction reaction mainly as following:[1]

$H_2O+1/2O_2+e=2OH^-$

Or near the anodic area:[1,39]

$Fe+OH^-=FeOH^-_{ad}$
$FeOH^-_{ad}=FeOH_{ad}+e$
$FeOH_{ad}+OH^-=Fe(OH)_{2s}+e$
$Fe(OH)_{2s}+OH^-=FeOOH_s+H_2O+e$
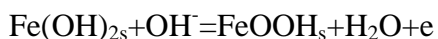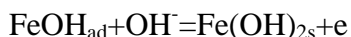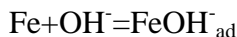
When inhibitor adsorb on carbon surface, the local area OH^- concentration will increase. Higher concentration of OH^- will restrain the reduction reaction equivalent to reverse direction or form oxide film in local area, which also inhibit the reduction and oxidation reaction.

5. CONCLUSIONS

1. The electrochemical measurements demonstrated that n-2OH-n (n=2,4,6,8,) could be thought as anodic retarder and steric covering inhibitor by forming an adsorption film in alkaline simulate concrete pore solution.

2. The increasing the adsorption atom and the carbon chain length can effectively increase the adsorption behavior and form compacted film barrier corrosion ion attack. The maximum of inhibition efficiency achieve at 99.4%.

3. The adsorption of 8-2OH-8 molecular corresponded well with Langmuir isotherm. The standard adsorption free energy is -40.97 $kJmol^{-1}$ in simulated concrete pore solution with 0.3 mol/l sodium chloride.

4. A reasonable interpretation about inhibition mechanism is given by data obtained from electrochemical experiments along with quantum chemical calculation and polarity compatibility. n-2OH-n (n=2,4,6,8) can form chemisorptions by N atom interaction with iron atom. Then non-polar carbon chain will near carbon steel surface or interlock with carbon chain each other by surface tension.

References

1. M. Valcarce, M. Vazquez. *Electrochim. Acta.,* 53 (2008) 5007.
2. S. Sawada, J. Kubo, C.Page, M.Page. *Corros. Sci.,* 49 (2007) 1186.
3. T. Soylev, M.Richadson. *Constr. Build. Mater.,* 22 (2008) 609.
4. F. Bolzoni, S. Goidanich, M. Ormellsese. Corros. Eng. Sci. Techn., 41 (2006) 212.
5. J. Lewis,C. Mason, D. Brereton. *Civil Engeering and Pulic Works Review,* 51 (1956) 881.
6. A.Rosenberg, J. Gaidis, T. Kossivas, R. Previte. *America Society for testing and materials,* Philadelphia, 1977, STP 629.
7. C. Alonso, C. Andrade, C. Argiz, B. Malric. *Cem. Conc. Res.,* 26 (1996) 405.
8. O.Rincon, O. Perez, E. Raredes, Y. Caldera, C. Urdaneta, I. Sandoval. *Cem. Conc. Comp.,* 24 (2002) 79.
9. B. Elsener, M. Buchuler, F. Stalder. *Corrosion*, 55 (1999)1155.
10. C. Monticelli, A. Frignani, G. Trabanelli. *Cem. Conc. Res.*, 30 (2000) 635.
11. J. Gaidis, *Cem. Conc. Compos.,* 26 (2004) 181.
12. C. Nmai. *Cem. Conc. Comp.*, 26 (2004) 199.
13. L. Zheng, H. Yang. *Acta Phys-Chim Sin.,* 26 (2010) 1354.
14. M. Mennucci, P. Bnaczek, P. Rodrgue, I. Costa. *Cem. Conc. Comp.,* 31 (2009) 418.
15. M. Ormellese, L. Lazzari, S. Goidanich, G. Fumagalli, A. Brenna. *Corros. Sci.,* 51 (2009) 2959.
16. M. Ameer, A. Fekry. *International Journal of Hydrogen Energy,* 35 (2010) 11387.
17. W. Morris, M. Vazquez. *Cem. Conc. Res.,*32 (2002) 259.
18. L. Fedrizzi, F. Azzolini, P. Bonora. *Cem. Conc. Res.,* 35 (2005) 551.
19. M. Ormellese, M. Berra, F. Bolzoni, T. Pastore. *Cem. Conc. Res.*, 36 (2006) 536.
20. R. Vedalakshmi, K. Rajagopaland, N Palaniswmy. Corros. Eng. Sci. Techn., 44 (2009) 20.
21. J. Tritthart. *Cem. Conc. Res.*, 2003, **33**, 829.
22. A. Welle, J. Liao, K. Kaiser, M. Grunze, U. Mader, N. Blank. *Appl. Surf. Sci.,* 119 (1997) 185.
23. H. Jamil, A. Shriri, R. Boulif, C. Bastos, M. Montemor, M. Ferreira. *Electrochim. Acta.,* 49 (2004) 2753.
24. X. Zhou, H. Yang, F. Wang. *Acta Phys–Chim Sin.,* 27(2011) 647.
25. J. Xu, L. Jiang, F.Xing. *Mater. Corros.,* 61 (2011) 802.
26. Z. Dong, T. Zhu, W. Shi, X.Guo. *Acta Phys-Chim Sin.,* 27 (2011) 905.
27. X.Zhou, H. Yang, F. Wang. *Corros. Sci.,* 54 (2012) 193.
28. Y. Magidson, M. Rubtsov. *J. Gen. Chem.(USSR),* 7 (1937) 1896.
29. G. Gao, C. Liang, H. Wang. *Corros. Sci.,* 49 (2007) 1833.
30. G. Gao, C. Liang. *J. Electrochem. Soc.*, 154 (2007) 144.
31. J. Liu, C. Chen, J. Cai, J. Liu, G.Cui. *Mater. Corros.,* 2012 (in press)
32. R. Yang, Y. Guo, F. Tang, X. Wang, R. Du, C. Lin. *Acta Phys-Chim Sin.,* 28 (2012) 1923 .
33. C. Cao. Corrosion Electrochemical Theory. 2nd Ed., Beijing: Chemical Industry Press, 2004: 246-287
34. J. Landoulsi, M. Genet, C. Richard, K. Kirat, S. Pulvin, P. Rouxhet. *J. Colloid. Interface Sci.,* 318 (2008) 278.
35. R. Hasanov, M. Sadikoglu, S. Biligic. *Appl. Surf. Sci.,* 253 (2007) 3913.
36. B. Wang, M. Du, J. Zhang, C. Gao. *Corros. Sci.,* 53 (2011) 353.
37. G. Gece. *Corros. Sci.,* 50 (2008) 2981.
38. Y Yan, W. Li, L. Cai, B. Hou. *Electrochim. Acta,* , 53 (2008) 5953.
39. K. Ann, H. Song. *Corros. Sci.,* 49 (2007) 4113.